STAI 8.1

QUALITATIVE ASSESSMENT OF THE ACOUSTIC DISTURBANCE ENVIRONMENT IN THE NASA LaRC 20-Inch MACH 6 WIND TUNNEL

Thomas J. Horvath,
Scott A. Berry, and H. Harris Hamilton
NASA Langley Research Center
Hampton, Virginia

95th Supersonic Tunnel Association, International
April 29 - May 2, 2001 /Hampton, VA.

QUALITATIVE ASSESSMENT OF THE ACOUSTIC DISTURBANCE ENVIRONMENT IN THE NASA LaRC 20-Inch MACH 6 WIND TUNNEL

Thomas J. Horvath*, Scott A. Berry*, H. Harris Hamilton*
NASA Langley Research Center

Abstract

An experimental investigation was conducted on a 5-degreehalf-angle cone with a flare in a conventional Mach 6 wind tunnel to examine the effect of facility noise on boundary layer transition. The effect of tunnel noise was inferred by comparing transition onset locations determined from the present test to that previously obtained in a Mach 6 quiet tunnel. Together, the two sets of experiments are believed to represent the first direct comparison of transition onset between a conventional and a quiet hypersonic wind tunnel using a common test model. In the present conventional hypersonic tunnel experiment, adiabatic wall temperatures were measured and heat transfer distributions were inferred on the cone flare model at zero degree angle of attack over a range of length Reynolds numbers ($2x10^6$ to $10x10^6$) which resulted in laminar and turbulent flow. Wall-to-total temperature ratio for the transient heating measurements and the adiabatic wall temperature measurements were 0.69 and 0.86, respectively. The cone flare nosetip radius was varied from 0.0001 to 0.125-inch to examine the effects of bluntness on transition onset. At comparable freestream conditions the transition onset Reynolds number obtained on the cone flare model in the conventional "noisy" tunnel was approximately 25 %lower than that measured in the low disturbance tunnel.

Nomenclature

d	base diameter (in)
h	heat transfer coeff. (lbm/ft^2-sec), $q/(H_{aw}- H_w)$ where $H_{aw} = H_{t,2}$
H	enthalpy (BTU/lbm)
L_{ref}	reference length based on sharp tip model (in)
M	Mach number
P	pressure, psia
q	heat transfer rate (BTU/ft^2-sec)
q	dynamic pressure (psi)
R	radius (in.)
t	time (sec)
Re	unit Reynolds number (1/ft)
S_{ref}	reference area (in^2)
T	temperature (°F)
x	axial distance from cone apex (in.)
α	angle of attack (deg)
θ	cone half angle (deg)
ρ	density (lbm/in^3)
γ	ratio of specific

Subscripts

aw	adiabatic wall
b	base
f	flare
∞	free-stream conditions
n	model nose
s	surface quantity
T	transition onset
t, 1	reservoir conditions
2	stagnation conditions behind normal shock
w	wall

Introduction

Thermal effects resulting from boundary layer transition during hypersonic flight can represent an important constraint for optimum reentry vehicle design. Design strategies for aerospace vehicle Thermal Protection Systems (TPS) that include empirical methods derived from ground based measurements are generally considered conservative. This is based upon the fact that high disturbance levels in the freestream flow of conventional hypersonic ground based test facilities can cause transition to occur at lower values of Reynolds numbers than may actually take place in flight[1]. Quiet wind tunnel technologies developed at, and incorporated into, wind tunnels at the NASA LaRC in the 1980's and 1990's have clearly established the influences of noise on transition and have advanced our understanding of transition via stability experiments conducted in these facilities[2-7]. By eliminating the overpowering effects of tunnel noise, these studies conducted in the low disturbance supersonic facilities have shown that boundary layer transition develops from a linear growth of natural instabilities that can be modeled by linear theory.

Despite advances in quiet wind tunnel technology, relatively few of these low disturbance supersonic or hypersonic facilities exist. Those in existence today are typically deficient in Reynolds number relative to representative flight conditions, and are generally not operated in a manner conducive for aeroheating assessment/screening studies. Thus, conventional hypersonic wind tunnels continue to serve as the primary source for experimental data from which to develop empirical methods[8-11] for flight

* Aerospace Technologist, Aerothermodynamics Branch, NASA Langley Research Center, Hampton, VA.

Presented at the 95th Meeting of the Supersonic Tunnel Association International, Hampton, VA., April 29-May 2, 2001. The document herein is non referencable.

transition prediction. Furthermore, when transition bypass mechanisms (a term commonly used to identify transition modes which bypass the linear process) such as vehicle surface roughness are present, it has often been argued that facility noise from conventional tunnels has little effect. Experimental studies have suggested that while noise may have little effect for roughness heights large enough to be considered effective[12] (turbulence initiated immediately downstream of the roughness element site), there still may be an influence of wind tunnel noise on transition onset data derived from roughness that are less than effective[13-15].

Present day TPS technology suggests that boundary layer transition on reentry vehicles will continue to be roughness dominated. Traditional ceramic TPS tiles such as used on the Shuttle Orbiter often suffer launch-induced damage and/or develop protruding gap fillers. Both forms of local surface roughness have been responsible for the occurrence of early boundary layer transition in flight[16]. Stitching patterns found on thermal blankets produce another form of local roughness. Metallic TPS panels that were proposed for use on the X-33[9,17-18] could have been susceptible to thermally induced expansion/bowing producing roughness in the form of a wavy wall. Based upon experimental evidence[13-15] suggesting the susceptibility of less than effective roughness elements to acoustic disturbances, quantification of the conventional facility disturbance environment is essential.

The purpose of this paper is to present preliminary experimental results from a study that is part of a larger ongoing effort to assess the acoustic disturbance environment of the NASA LaRC 20-Inch Mach 6 Air Tunnel. This initial experimental study is considered qualitative and no attempt was made to measure freestream fluctuations. The relative disturbance environment of this conventional tunnel was expressed via differences in transition onset locations measured on a cone flare model previously tested in the LaRC Mach 6 Nozzle Test Chamber (NTC) Quiet Tunnel.

In the conventional hypersonic tunnel experiment two independent measurement techniques were used to identify transition onset. Adiabatic wall temperatures were measured and heat transfer distributions were inferred on the cone flare model at zero degree angle of attack over a range of length Reynolds numbers ($2x10^6$ to $10x10^6$) which resulted in laminar and turbulent flow. Wall-to-total temperature ratio for the transient heating measurements and the adiabatic wall temperature measurements were 0.69 and 0.86, respectively. The cone flare nosetip radius was varied from 0.0001 to 0.125-inch to examine the effects of bluntness on transition onset. Transition onset locations inferred from the present test were compared to onset locations previously determined from tests in the Mach 6 NTC Quiet Tunnel. Together, the two sets of experiments are believed to represent the first direct comparison of transition onset between a conventional and quiet hypersonic wind tunnel using a common test model at comparable freestream conditions.

Experimental Methods

Model

Details of the cone flare model (designation 93-10) originally built and instrumented for testing in the LaRC Mach 6 NTC Quiet Tunnel can be found in Ref. 3. A schematic diagram of the model geometry is shown in Fig. 1. Measuring 20-inches in length (sharp tip) the model base diameter is 4.6-inch. The first 10-inch section of the model consists of a 5 degree half angle cone followed by a 10-inch section comprised of an outward flare. Tangency was specified at the cone flare junction. An arc radius of 93.07-inches defined the flare curvature. As discussed in Ref. 3, the purpose of the flare was to promote boundary layer instability via an adverse pressure gradient to insure transition would occur on the model within the limited quiet flow Reynolds number capability of the Mach 6 NTC Quiet Tunnel.

The 15-5 stainless steel model was constructed with a thin wall to reduce surface heat conduction effects and to bring the model to thermal equilibrium as quickly as possible during a run. The model was constructed with five interchangeable nosetips (R_n= 0.0001, 0.03125, 0.06250, 0.09375, and 0.125-inch) fabricated from 13-8 stainless steel (see Fig. 2a). The surface finish was originally highly polished to minimize effects on the model boundary layer stability and, for the present test, appeared to be free of large surface scratches (despite several entries into the quiet tunnel and the subsequent long-term storage).

Model Instrumentation

A total of fifty-one type K thermocouples were tack welded to the model thin wall backside along a single ray. The thermocouples were spaced axially along this ray at 1-inch intervals between model stations x=2 and 9 inches and 0.25-inch intervals from model stations x=9 to 19.75-inches. The local model wall thickness was nominally 0.030-inch along the location of the streamwise row of thermocouples and 0.060-inch elsewhere. Twenty-nine 0.040-inch diameter static pressure orifices were located on the opposite side of the model.

Facility Descriptions

Although the Mach 6 NTC Quiet Tunnel has since been disassembled, at the time of the original quiet tunnel experiments, both facilities were located within the same lab and shared a common air supply line and heater element. For a short period, both were managed under the Aerothermodynamic Facilities

Complex (AFC). This complex presently consists of 4 hypersonic wind tunnels that represent a large fraction of the nation's conventional aerothermodynamic test capability. Collectively, they provide a wide range of Mach number, unit Reynolds number, and normal shock density ratio [19]. This range of hypersonic simulation parameters is due, in part, to the use of two different test gases (air, and tetraflouromethane), thereby making the facilities unique national assets. The AFC facilities are relatively small and economical to operate, hence ideally suited for fast-paced aerodynamic performance and aeroheating, and transition studies aimed at screening, assessing, optimizing, and bench-marking (when combined with computational fluid dynamics) advanced aerospace vehicle concepts and basic fundamental flow physics research.

20-Inch Mach 6 Air Tunnel: Heated, dried, and filtered air is used as the test gas. Typical operating conditions for the tunnel are: stagnation pressures ranging from 30 to 500 psia; stagnation temperatures from 760-deg to 1000-degR; and freestream unit Reynolds numbers from 0.5 to 8 million per foot. A two-dimensional, contoured nozzle is used to provide nominal freestream Mach numbers from 5.8 to 6.1. The test section is 20.5 by 20 inches; the nozzle throat is 0.399 by 20.5-inch. A bottom-mounted model injection system can insert models from a sheltered position to the tunnel centerline in less than 0.5-sec. Run times of up to 15 minutes were achieved for the adiabatic wall temperature measurements. For the transient heat transfer tests, the model residence time in the flow was limited to 20 seconds. A detailed description of this facility may be found in Ref. 19

In an attempt to attenuate noise from upstream piping/air control valves, the settling chamber was recently retrofitted with a series of acoustically damping porous screen elements. This technology was based upon quiet tunnel experience at LaRC and was designed to reduce pressure fluctuations in the settling chamber to approximately 0.005 % of the stagnation pressure.

Mach 6 Nozzle Test Chamber Quiet Tunnel: Heated and dried air was used as the test gas. Typical low disturbance operating conditions for the tunnel were: stagnation pressures ranging from 80 to 130 psia, stagnation temperatures up to 810R, and a maximum freestream unit Reynolds numbers of 2.8 million per foot. A contoured axisymmetric slow expansion nozzle was used to provide a nominal freestream Mach number of approximately 5.9. The nozzle exit diameter was 7.49 inches with the flow exhausting into an open jet test section; the nozzle throat diameter was 1.0-inch. This facility had no model injection system. Run time for the adiabatic wall temperature measurements varied between 30 and 60 minutes. Details concerning the facility, the size of the quiet flow envelope and measurements of the disturbance environment are discussed in Ref. 20.

Test Conditions and Setup

Reservoir and corresponding free stream flow conditions for the present tests in the LaRC 20-Inch Mach 6 Air Tunnel are presented in Table 1. The freestream properties were determined from the measured reservoir pressure and temperature and the measured pitot pressure at the test section. The standard procedure used to compute flow conditions for the AFC facilities uses the viscosity formulation given by Chapman-Cowling and is detailed in Ref. 21. For the present test, the computed Reynolds number was based upon Sutherland's formulation for viscosity to maintain consistency with the method employed to compute quiet tunnel conditions.

In the present test, the ratio of model base area to tunnel cross sectional area for the flared cone model was 0.04. In both wind tunnel experiments a base mounted cylindrical sting supported the cone flare model. Model angle-of-attack and sideslip were set to zero in the tunnel using a combination of an inclinometer and a laser alignment system. A photograph of the ting supported model is shown in Fig. 2b. Details of the model installation in the NASA LaRC Mach 6 NTC Quiet Tunnel can be found in Ref. 3.

Test Techniques

Adiabatic wall temperature: In the original stability experiments conducted in the low disturbance tunnel, the individual thermocouple temperature measurements were monitored with time and used to determine when the model had obtained a state of thermal equilibrium. The resulting temperature distribution was used to identify transition onset. The test procedure for the quiet tunnel measurements involved preheating the model by exposing it to hypersonic conditions for 30 to 60 minutes to achieve thermal equilibrium. For the adiabatic wall temperature measurements in the conventional tunnel test, the test procedure was designed to approximate as closely as possible this technique. That is, the model was injected into the hypersonic stream and allowed to thermally equilibrate. Higher mass flow rates with the present conventional tunnel tests limited total run times to approximately 12 to 15 minutes depending on the desired Reynolds number. Temperature time histories obtained during each run were monitored and indicated when thermal equilibrium was achieved. The model was not allowed to cool between runs in order to accelerate the time required to reach thermal equilibrium on subsequent runs.

Transient thin skin heat transfer: The thin wall construction of the cone flare model made it

possible to apply the transient thin skin calorimetery measurement technique to infer heat transfer distributions along the streamwise array of thermocouples. The lack of a model injection system and placement of the model inside the nozzle prevented this type of heating technique to be exploited in the low disturbance tunnel. In the current conventional tunnel test, separate tunnel runs were required to obtain transient heating data and adiabatic wall temperature data. For the transient technique, the hypersonic stream conditions were established with the model in a sheltered position. The model was then injected into the flow and thermocouple temperature time histories were acquired. The model was allowed to cool between runs in order to obtain isothermal conditions necessary for the calculation of heat transfer.

Surface static pressure: Surface pressure measurements were obtained concurrent with the adiabatic wall temperature or heat transfer data and were made with an electronically scanned pressure (ESP) transducer. The full-scale range of the absolute pressure transducer was 0.36 psia. The long run times associated with the adiabatic wall temperature measurements provided more than adequate time for settling. The relatively short test times associated with the transient heating measurements did not provide enough settling time.

Flow Visualization: Flow visualization in the form of schlieren was used to complement the surface temperature and heating measurements. The LaRC 20-Inch Mach 6 Air Tunnel is equipped with a pulsed white-light, Z-pattern, single-pass schlieren system with a field of view encompassing the entire test core. The model length did not permit an entire view of the cone flare length. The light source was pulsed for approximately a 3 ms duration. Images were recorded on a high-resolution digital camera and will be enhanced with commercial software for future analysis.

Data Reduction and Uncertainty

A 16-bit analog-to-digital facility acquisition system was used to acquire data. The facility, model thermocouple, and pressure data was collected by this system at a rate of 50 samples per second over a 20 second interval during each run. The raw data was transferred to a Hewlett-Packard 9000 computer for data reduction and storage.

Thermocouple mV output was referenced to an electronic ice point and was converted to engineering units via a standard type K lookup table. Accuracy of the surface temperature measurement is believed to be better than ±5 degrees. Heating rates under transient conditions were calculated from backside surface temperature measurements as discussed in detail in Ref. 22. The inferred heating rates were normalized to a theoretical reference value. The model was originally designed to measure adiabatic wall temperatures and wall thickness measurements critical for inferring accurate heating magnitudes for CFD benchmarking were not documented. However, as the goal of the present test was the determination of transition onset, the heating distribution trends were more than adequate for indicating the departure from a reference laminar boundary layer state. For the transient thin skin heating measurements, the overall experimental uncertainty is believed to be better than ±20%. Conduction effects near the model base may have contributed to a larger uncertainty in this region. Repeatability for the normalized laminar heat transfer measurements was found to be generally better than ±4%.

The ESP pressure measurement system was calibrated prior to each run. The measured surface pressure was expressed in nondimensional form, P_s/P_∞, and in terms of a pressure coefficient. Measured reservoir values of $P_{t,1}$ and $T_{t,1}$ are believed to be accurate to within ±2 percent. Uncertainties in model angle-of-attack and sideslip are believed to be ±0.1 degree.

Results and Discussion

Conventional Tunnel

Normalized surface pressure distribution for the sharp tip (R_n=0.0001-inch) at Re_L=4.8 x 10^6 is shown in Fig. 3. The flare section produced a nearly constant adverse pressure gradient. While not the focus of the present analysis, the nondimensional pressure gradient magnitude $[d(P_s/P_\infty)/d(X/L)]$ from the present test was within the range produced by a family of cones tested to examine the effects of favorable and adverse pressure gradients on transition zone length[23]. The value of the nondimensional pressure gradient $[d(P_s/P_\infty)/d(X/L)]$ on the flare section was obtained by linear regression of the data and calculated to be 3.3. As expected, the pressure coefficient (not shown) distribution along the entire model was in agreement with previous quiet tunnel pressure measurements reported in Ref. 6.

Normalized heat transfer distributions for the sharp tip (R_n=0.0001-inch) cone flare model are presented in Fig. 4, over the length Reynolds number (Re_L) range 2.0 x 10^6 to 10.3 x 10^6. The onset of boundary layer transition at any given Reynolds number has been interpreted as the departure from the laminar distribution measured for the Re_L=2.0 x 10^6 condition. The collapse of the heating distributions with Reynolds number on the cone section and onto the flare indicated the presence and extent of laminar flow. The onset of transition was observed for Re_L=3.8 x 10^6 on the flare section and progressively moved forward onto the straight cone section with increasing Reynolds number. The transition zone

extended to the base of the flare at Re_L=3.8 x 10^6 and 4.8 x 10^6. At the higher length Reynolds numbers, Re_L=7.5 x 10^6 and 10.3 x 10^6, transition onset moved onto the straight cone section; this suggests that the initial instability and growth occurred in the zero pressure gradient region. The heat transfer at the higher Reynolds numbers exhibited the same classic transitional overshoot and subsequent relaxation to turbulent levels as the cone flares results of Ref. 23.

After many years of testing and handling, the quality of the sharp nosetip (R_n=0.0001-inch) was initially a concern. As a second (backup) sharp nosetip was available, measurements on it were also obtained. Transition onset locations very consistent with the original sharp tip were measured and have alleviated concerns as to condition of the leading edge radius.

The model wall temperature under adiabatic conditions was, naturally, higher than that measured under the transient heating technique. This difference in surface temperature is shown in Fig. 5, for reservoir conditions selected to match those achieved in the quiet tunnel (Re_L=4.8 x 10^6). The backside wall temperature distribution along the cone flare obtained 1.5 seconds after model exposure was essentially constant (T_w=95 deg. F; T_w/T_t=0.69). At the same Reynolds number under adiabatic conditions the wall temperature was higher (250 deg. F; T_w/T_t=0.86) with surface temperature increases (310 deg. F; T_w/T_t=0.95) associated with boundary layer transition. A stability analysis of the quiet tunnel cone flare results[24] has indicated that a variable wall temperature distribution at adiabatic conditions produced little effect on the instability amplification rates on the model. The theoretical results of Ref. 24 also indicated that an increase in wall-to-total temperature ratio from 0.51 to 0.86 would increase the frequency of the most amplified first and second mode disturbances. The calculated second mode frequencies were considered high (260kHZ range) and no conclusion was reached as to whether or not they could be excited by freestream disturbances in a given environment.

Despite the wall-to-total temperature differences in the present test, the two methods for determining transition onset yielded equivalent locations as shown in Fig. 6, (representative of comparisons of transition onset for all Reynolds numbers). The onset point from the transient heating distributions clearly indicated a departure from laminar heating (Re_L=2.0 x 10^6) on the flare section at x=12.2-inches. The method for estimating transition onset via the adiabatic wall temperature consisted of determining the intersection of two straight lines passing through the laminar region and the sharp temperature rise region as discussed in Ref. 3. While more subjective in nature, the onset locations agree remarkably well. Differences in the wall to total temperature ratio of 0.69 and 0.86 had little, if any, impact on the location of transition onset whether it occurred on the straight cone or flare section.

While primarily intended to provide data for comparison to the quiet tunnel results, the present conventional tests also served to assess the effects of nose bluntness on transition onset. The effect of nose bluntness at Re_L=3.8 x 10^6 is shown in Fig. 7. As expected, nosetip bluntness delayed boundary layer transition. Transition onset for the sharp tip (R_n=0.0001-in.) occurred at x=14-inches with the transition zone extending to the end of the model. An increase in the nosetip radius to 0.125-inches stabilized and extended the laminar boundary layer to the end of the model.

Comparison to Quiet Tunnel

A direct comparison of conventional vs. quiet tunnel transition onset locations at adiabatic wall conditions for comparable reservoir and freestream conditions is shown, Fig. 8, for Re_L=4.8 x 10^6. To the author's knowledge this represents the first comparison of transition onset location between a conventional and low disturbance hypersonic tunnel utilizing a common model. The transition onset Reynolds number (Re_T -based on the length to transition onset) as measured in the conventional tunnel was 23% lower than that inferred from the low disturbance tunnel. Prior to this direct comparison, the influence of acoustic disturbances on flare cone hypersonic transition was conservatively estimated by running the quiet tunnel in a "noisy" mode (diverter valves normally open to promote a laminar nozzle wall boundary layer are closed resulting in a turbulent nozzle boundary layer). In the "noisy" mode of the low disturbance tunnel, transition onset occurred earlier than that measured in the conventional tunnel. Interpretation of the data presented in Ref. 3 yielded a 42% reduction in the cone flare transition onset Reynolds number when the Mach 6 low disturbance tunnel was operated in the noisy mode as compared to the 23% reduction via a conventional facility.

Measurements on sharp cones performed in supersonic quiet tunnels typically yield values of Re_T that are two to three times the values obtained in conventional tunnels (and nearly an order of magnitude for flat plates)[25]. While this may be valid at M=3.5 for sharp cones, the present cone flare tests at M=6 do not exhibit such a level of disparity between a conventional and a low disturbance tunnel. Recognition of the presence of different instability modes and the influence of Mach number are equally important parameters to consider.

The reservoir temperature and pressure conditions for the quiet tunnel condition were 350 deg F and 130 psia, respectively. This relatively low temperature reservoir condition had been selected to reduce hot-wire overheat requirements for that test

series. Concerns that this quiet tunnel operating condition lie too close to the air liquefaction curve were addressed in the conventional tunnel by testing at different reservoir pressure/temperature combinations so as to hold Re_L fixed. No measurable effect on transition onset Reynolds number were observed (not shown).

Transition onset for cones and flat plates at supersonic conditions (taken from Ref. 2) with the present cone flare data are plotted against unit Reynolds number in Fig. 9. Also included is unpublished flat plate transition data recently obtained in the conventional LaRC 20-Inch Mach 6 Air Tunnel. The Mach 6 cone flare and flat plate data obtained in a conventional hypersonic tunnel exhibit the, so-called, unit Reynolds number effect whereby radiated noise intensity from the tunnel wall boundary layer varies with Reynolds number and dominates the smooth body transition process. As expected, the present data also show that the cone flare transition onset Reynolds number was higher than the flat plate data for a given unit Reynolds number. This trend, commonly observed in conventional facilities, is contrary to that measured in supersonic quiet tunnels and to that predicted by stability theory. As discussed in Ref. 2, this may be due to the faster boundary layer growth on a flat plate relative to a cone and thus, stronger receptivity of the flat plate to the incident acoustic field (in the conventional tunnel). The flat plate transition onset Reynolds numbers from the conventional LaRC Mach 6 tunnel are consistently higher than the flat plate M=3 and 3.7 data from the AEDC and JPL facilities. Since it has been shown that the disturbance field sound intensity correlates with test section size[26] one might expect better agreement of the present smooth flat plate Re_T data to the JPL results. Despite the similar test section dimensions to the JPL tunnel, other factors such as Mach number effects on radiated tunnel wall noise, boundary layer stability on the cone flare, or the noise reduction technology in the conventional tunnel settling chamber appears to have an influence on Re_T.

Concluding Remarks

Despite advances in supersonic/hypersonic quiet wind tunnel technology, relatively few of such low disturbance facilities exist. Those in existence today are typically deficient in Reynolds number relative to representative flight conditions, and are generally not operated in a manner conducive for aeroheating assessment/screening studies. Thus, conventional hypersonic wind tunnels continue to serve as the primary source for experimental data from which to develop empirical methods for flight transition prediction. When transition bypass mechanisms such as vehicle surface roughness are present it has often been argued in the past that facility noise has little effect. Recent studies have indicated that quantification of the disturbance environment in a conventional hypersonic tunnel is essential even when boundary layer transition bypass mechanisms, such as surface roughness, are present.

The purpose of the present study was to present preliminary experimental results from a study that is part of a larger ongoing effort to assess the acoustic disturbance environment of the NASA LaRC 20-Inch Mach 6 Air Tunnel. An experimental investigation was conducted on a 5-degree half angle cone with a flare in a conventional Mach 6 wind tunnel to examine the effect of facility noise on boundary layer transition. The effect of tunnel noise was inferred by comparing transition onset locations determined from the present test to that previously obtained in a Mach 6 quiet tunnel. Together, the two sets of experiments are believed to represent the first direct comparison of transition onset between a conventional and quiet hypersonic wind tunnel using a common test model. At comparable freestream conditions the transition onset Reynolds number obtained on the cone flare in the conventional "noisy" tunnel was approximately 25% lower than that measured in the low disturbance tunnel.

Acknowledgments

Without the assistance of the following individuals this work would not have been possible: Steve Wilkinson, Charlie Greenhalgh, and Kevin Meidinger for model design information and model refurbishment; John Ellis, Grace Gleason, Rowland Hatten, and Steve Jones for wind tunnel support; Sheila Wright and Mike Difulvio for data acquisition assistance; Steve Wilkinson and Brian Hollis for analysis support; and Richard Wheless for documentation assistance. The authors gratefully acknowledge their contributions and behind-the-scenes work.

References

1. Beckwith, I. E., and Miller, C. G., "Aerothermodynamics and transition in High Speed Wind Tunnels at NASA LaRC," Annual Reviews of Fluid Mechanics, Vol. 22, 1990.

2. Beckwith, I. E., Chen, F.J., and Malik, M. R., "Transition Research in the Mach 3.5 Low-Disturbance Wind Tunnel and Comparisons of Data with Theory," SAE 892379, Sept., 1989.

3. Lachowicz, J. T., and Chokani, N., "Hypersonic Boundary Layer Stability Experiments in a Quiet Wind Tunnel with Bluntness Effects," NASA CR 198272, Jan., 1996.

4. Blanchard, A. E., and Selby, G. V., "An Experimental Investigation of Wall-Cooling Effects on Hypersonic Boundary Layer Stability in a Quiet Wind Tunnel," NASA CR 198277, Feb., 1996.

5.Doggett, G. P., and Chokani, N., "Hypersonic Boundary Layer Stability Experiments on a Flared-Cone Model at Angle of Attack in a Quiet Wind Tunnel," NASA CR 201617, Oct., 1996.

6.Doggett, G. P., Chokani, N., and Wilkinson, S. P., "Hypersonic Boundary Layer Stability Experiments on a Flared-Cone Model at Angle of Attack in a Quiet Wind Tunnel," AIAA Paper 97-0557, Jan., 1997.

7.Chokani, N., "Perspective: Stability Experiments at Hypersonic Speeds in a Quiet Wind Tunnel," AIAA Paper 2001-0211, Jan., 2001.

8.Berry, S. A., Bouslog, S. A., Brauckmann, G. J., and Caram, J. M., "Shuttle Orbiter Experimental Boundary-Layer Transition Results with Isolated Roughness," *Journal of Spacecraft and Rockets*, Vol. 35, No. 3, 1998, pp. 241-248.

9.Berry, S. A.,, Horvath, T. J., Hollis, B. R., Thompson, R. A., and Hamilton, H. H., "X-33 Hypersonic Boundary Layer Transition," AIAA Paper 99-3560, June 1999.

10.Horvath, T. J., Berry, S. A., Merski, N. R., and Fitzgerald, S. M., "X-38 Experimental Aerothermodynamics," AIAA Paper 2000-2685, June, 2000.

11.Berry, S. A., Auslander, A. H., Dilley, A. D., and Calleja, J. F., "Hypersonic Boundary-Layer Trip Development for Hyper-X," AIAA Paper 2000-4012, August, 2000.

12.Poll, D. I., "Laminar-Turbulent Transition," AGARD Advisory Report 319, Vol.1, 1996.

13.Takeshi, I., Randall, L. A., and Schneider, S. P., "Effect of Freestream Noise on Roughness-Induced Boundary-Layer Transition for a Scramjet Inlet," AIAA Paper 2000-0284, Jan, 2000.

14.Dietz, A. J., "Boundary-Layer Receptivity to Transient Convected Disturbances" AIAA Journal, Vol. 36,No. 7, July, 1998.

15.Schneider, S. P., "Effects of High-Speed Tunnel Noise on Laminar-Turbulent Transition", AIAA Paper 2000-2205, June 2000.

16.Bouslog, S. A., An, M. Y., and Derry, S. M., "Orbiter Windward-Surface Boundary-layer Transition Flight Data," NASA CP 3248 Part 2, April, 1995.

17.Bouslog, S.A., Moore, B., Lawson, I., and Sawyer, J. W., "X-33 Metallic TPS Tests in NASA-LaRC High Temperature Tunnel," AIAA Paper 99-1045, Jan. 1999.

18.Palmer, G., Kontinos, D., and Sherman, B., "Surface Heating Effects of X-33 Vehicle TPS Panel Bowing, Steps, and Gaps," AIAA Paper 98-0865, Jan. 1998.

19.Miller, C. G., "Langley Hypersonic Aerodynamic/Aerothermodynamic Testing Capabilities - Present and Future," AIAA Paper 90-1376, June 1990.

20.Blanchard, A. E., Lachowicz, and Wilkinson, S. P., "NASA Langley Mach 6 Quiet Wind-Tunnel Performance," AIAA Journal, Vol. 35, No. 1, January 1997.

21.Hollis, B. R., "Real-Gas Flow Properties for NASA Langley Research Center Aerothermodynamic Facilities Complex Wind Tunnels," NASA CR 4755, Sept., 1996.

22.Miller, Charles G. III, "Comparison of Thin-Film Resistance Heat-Transfer Gages With Thin-Skin Transient Calorimeter Gages in Conventional Hypersonic Wind Tunnels," NASA TM 83197, Dec., 1981.

23.Kimmel, R. L., "The Effect of Pressure Gradients on Transition Zone Length in Hypersonic Boundary Layers," Journal of Fluids Engineering, Vol. 119, March, 1997.

24.Balakumar, P. and Malik, M. R., "Effects of Adverse Pressure Gradient and Wall Cooling on Instability of Hypersonic Boundary Layers," High Technology Report HTC-9404, March, 1994.

25.Arnal, D., "Boundary Layer Transition: Predictions Based on Linear Theory," AGARD R-793, April, 1994.

26.Pate, S. R., "Dominance of Radiated Aerodynamic Noise on Boundary –Layer Transition in Supersonic-Hypersonic Wind Tunnels," AEDC-TR-77-107, March, 1978.

Table 1: Flow Conditions

Facility	M_∞	q_∞(psi)	$P_{t,1}$(psi)	$T_{t,1}$(°F)	ρ_2/ρ_∞	Re_∞/ft (x10^6)
20-In Mach6 Air	5.88	1.08	62	417	5.24	1.20
	5.94	2.15	129	446	5.27	2.30
	5.94	2.29	134	347	5.26	2.89
	5.98	4.10	254	443	5.26	4.48
	6.00	5.87	369	469	5.27	6.17

Shaded conditions represent a match to Mach 6 NTC Quiet Tunnel reservoir conditions

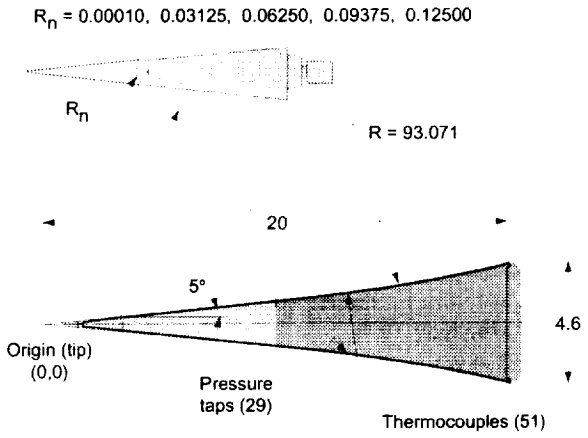

Fig. 1. Model 93-10 flared cone model and nosetip dimensions (inches)

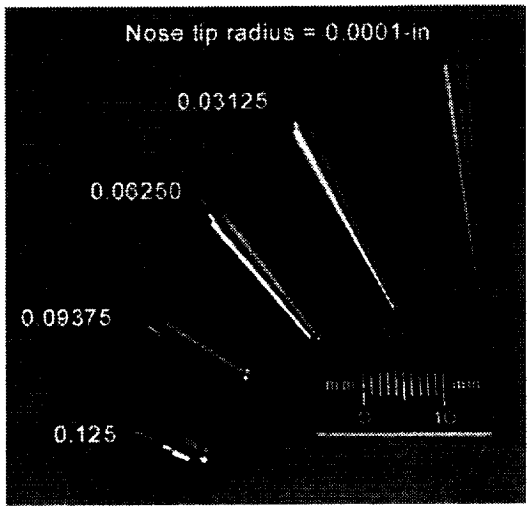

Fig. 2a. Flared cone model interchangable nosetips

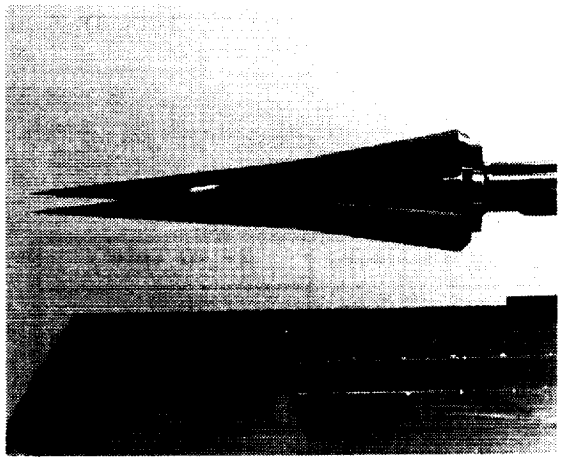

Fig. 2b. Flared cone model installation in the NASA LaRC 20-Inch Mach 6 Tunnel

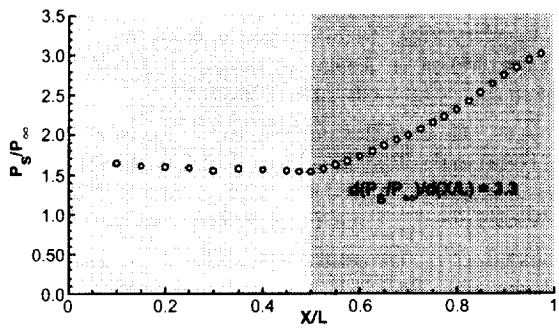

Fig. 3. Static surface pressure distribution, M_∞=6, Re_L=4.8 x 10^6, α=0 deg, R_n=0.0001-in.

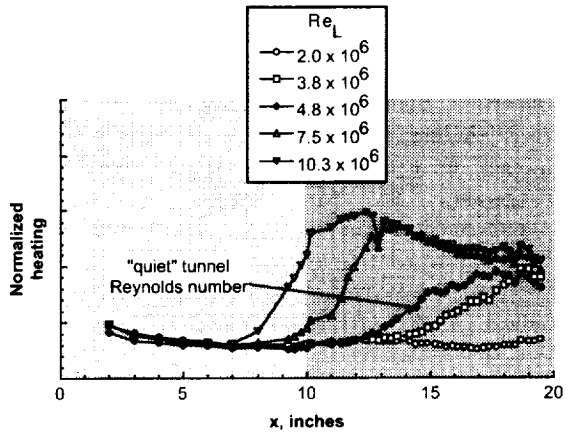

Fig. 4. Reynolds number effect on transition onset location as inferred from transient heating distributions, M_∞=6, α=0 deg, R_n=0.0001-in.

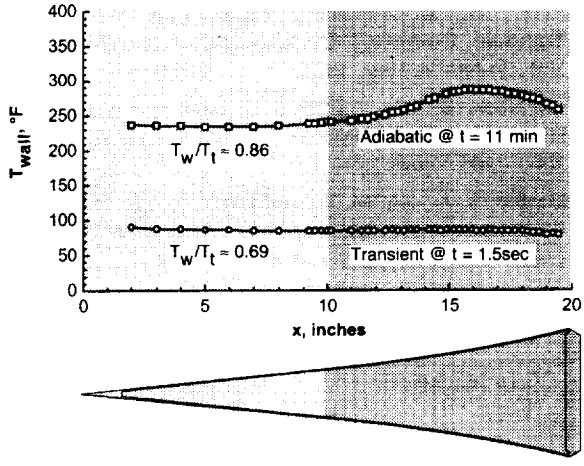

Fig. 5. Comparison of adiabatic wall temperature distribution with transient measurement, M_∞=6, Re_L=4.8 x 10^6, α=0 deg, R_n=0.0001-in.

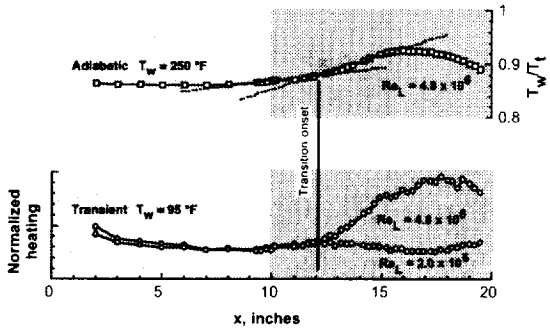

Fig. 6. Comparison of transition onset location as inferred from adiabatic wall temperature and transient heating distributions, M_∞=6, Re_L=4.8 x 10^6, α=0 deg, R_n=0.0001-in.

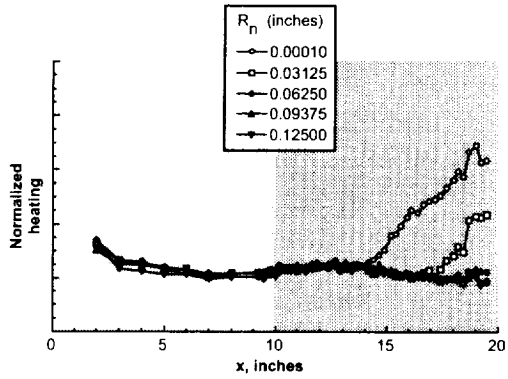

Fig. 7. Effects of nosetip bluntness on transition onset location as inferred from transient heating distributions, M_∞=6, Re_L=3.8 x 10^6, α=0 deg

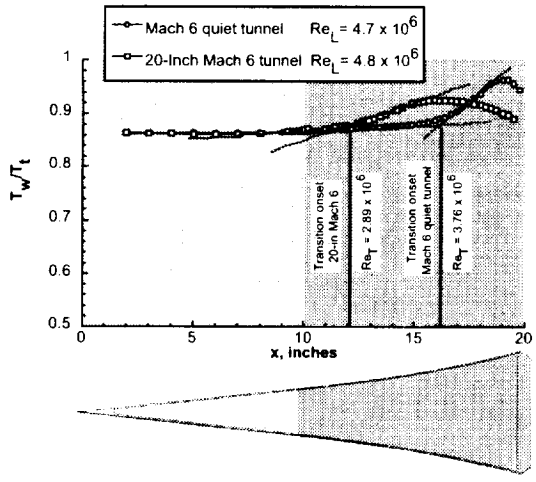

Fig. 8 Comparison of conventional and quiet tunnel transition onset location as inferred from adiabatic wall temperature distributions, M_∞=6, Re_L=4.8 x 10^6, α=0 deg, R_n=0.0001-in.

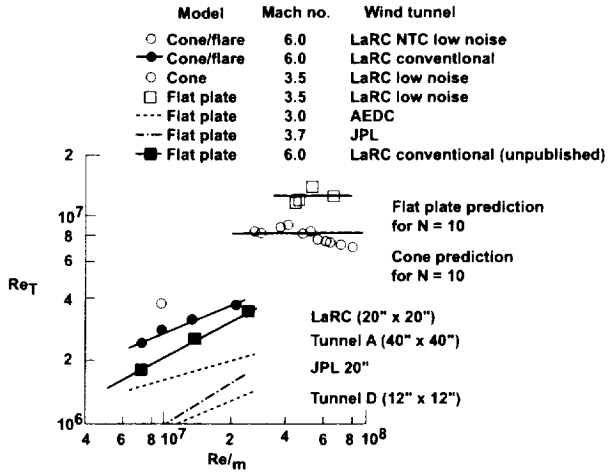

Fig. 9. Comparison of transition onset Reynolds numbers on cone and flat plates with present data [Ref. 2].